CILAMCE 2017
Florianópolis - Santa Catarina - Brazil

ANALYSIS OF A DISTANCE MEASUREMENT SYSTEM BASED ON MONOCULAR CAMERA

Rodrigo Adamshuk Silva

David Carvalho Andrade

Felipe Rezende Franco

Felipe Bueno

Max Mauro Dias Santos

Sérgio Okida

rodrigo.adk@gmail.com

davidcarvalho1992@hotmail.com

felipefranco@alunos.utfpr.edu.br

rsbueno.felipe@gmail.com

maxmaurodias@hotmail.com

sergiookida@utfpr.edu.br

Universidade Tecnológica do Paraná – Campus Ponta Grossa (UTFPR-PG)

Avenida Monteiro Lobato s/n km04, 84016-210, Paraná, Ponta Grossa, Brazil

Abstract. *Collision mitigation is an automotive function that enables to measure the distance of an object and alerts the driver to take preventive measures and avoid accidents. This work presents a strategy able to evaluate an ahead vehicle distance based on the monocular camera. The Inverse Perspective Method is applied to measure the distance. The strategy was evaluated for a flat highway, with a vehicle positioned at distances between 10 and 50 meters from the camera, the measurements were taken every 5 m. The images we acquired in three periods of the day, in the mid-day, in the mid-afternoon and the evening. The mean error obtained ranged from 2.87% to 18.43% of the value accepted as true. By the Analysis of Variance (ANOVA), we verified that the average of the distances calculated in the three periods of the day is significantly different. These errors caused by the environmental lighting conditions, the positioning of the vehicle relative to the light source, which produced different types and sizes* *of shadows that interfere with vehicle detection system. The purposed distance measurement system presented satisfactory results. However, it is necessary the development of more robust methods to remove the influence of environmental conditions.*

Keywords: *Distance measurement system, Monocular camera, Inverse Perspective Mapping Method, Collision mitigation*

1 INTRODUCTION

According to the World Health Organization (2015), about 1.2 million people die worldwide every year due to traffic accidents. Most of the deaths occurred in low and middle-income countries, where rapid economic development promoted vehicle sales, contributing to an increase in the number of traffic accidents.

In 2014, according to the report "TRAFFIC ACCIDENTS ON BRAZILIAN FEDERAL HIGHWAYS", occurred 169,163 accidents of which 8,227 people died, and about 100,000 were injured. The rear-end collision and the trampling of people represented, respectively, 29.2% and 14.6% of the accidents, 18.2% and 3.9% of injuries and has been responsible for the almost 8.4% and 14.6% of deaths (Ipea, 2015).

These traffic accidents due to distraction, error in the estimation of the distance of an object in the lane, fatigue and other factors stimulate the development of systems to assist drivers in risk situations. One of these automotive functions is collision mitigation that measures the distance to an object and alerts the driver to take preventive measures and avoid accidents, thereby reducing the number of deaths, injuries, and material damages.

Among the several methods used to estimate the distance between the vehicle and an object are millimeter-wave RADAR, LIDAR, ultrasonic ranging and infrared ranging and computer vision. Zhao et al. (2015) present the principle of operation, the applications as well as the advantages and shortcomings of each of these methods, given particular attention for computer-vision methods because of their accuracy in recognizing objects. The stereo vision that use two video cameras to see the same scene has been applied in automotive industry to develop collision mitigation system due to their ability in determining distances and object sizes (Nedevschi et al., 2004; Bosch, 2012). However, due the complexity and costs of the stereo vision systems, monocular cameras approaches to measure distances have been proposed (Tuohy et al., 2010).

In this work, we present a strategy able to evaluate an ahead vehicle distance based on a monocular camera installed in a vehicle windshield. The purposed system consists of the stages of image acquisition, preprocessing, camera parameter estimation, object detection, and distance determination. After calibrating the distance measurement method, we evaluated it on a flat highway and at different times of the day, in the mid-day, in the mid-afternoon and the evening.

This paper is organized as follows: section 2 describes the method used to correct the perspective effect; section 3 presents the strategy for measure the distance; section 4 evaluate the method and make a discussion about the results, and section 5 presents the conclusion.

2 INVERSE PERSPECTIVE MAPPING (IPM)

The projection of points from three-dimensional world $W = \{(x, y, z)\}$ on a plane $I = \{(r, c)\}$, performed by the camera during the image acquisition process (Fig. 1.a), produces perspective distortion. Figure 1.b shows this perspective effect, note that the width of the highway changes according to the distance from the camera, although the lanes of the highway are parallel (Broggi, 1995).

Proceedings of the XXXVIII Iberian Latin-American Congress on Computational Methods in Engineering
P.O. Faria, R.H. Lopez, L.F.F. Miguel, W.J.S. Gomes, M. Noronha (Editores), ABMEC, Florianópolis, SC, Brazil, November 5-8, 2017.

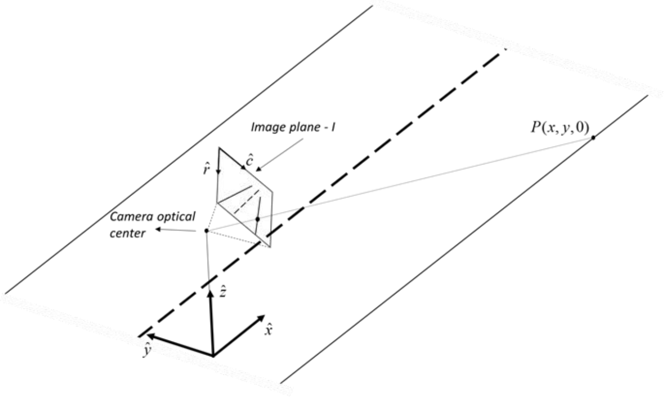

(a) **(b)**

Figure 1. (a) Projection of a point P from the 3D world on the image plane *I* and (b) The perspective effect, note that the width of the highway changes according to the distance.

Due to the perspective effect, each pixel in the image plane represents a portion of the highway with different size (Bertozzi et al., 1998). Pixels away from the camera represent larger areas of the highway than pixels close to it (Fig. 2). Therefore, to measure distances is necessary to correct this distortion, which is done through the inverse perspective mapping method (IPM). The IPM remaps the pixels of the image in perspective to a different position creating a new bi-dimensional image, similar to an aerial view of the highway.

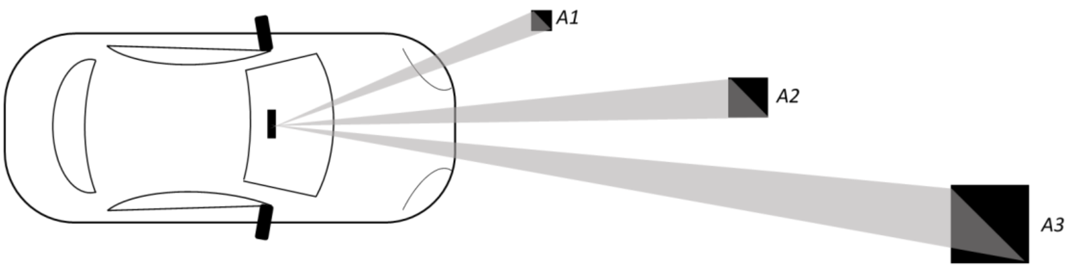

Figure 2. The perspective effect. The figure represents three road portions with different areas (A3>A2>A1) where each is represented by a single pixel of the image.

Johnson & Hamburger (2007) shows in details the algebraic and trigonometric manipulations necessary to mapping from the image plane to the world ($f : I \rightarrow W$). To get the aerial view is assumed that z is equal a zero. Figure 3 represents the lateral, and top views of the highway showed in Fig. 1.a where the parameters necessary to compute the IPM are: (Cario et al., 2009; Silva et al., 2017)

- h - the height of the camera optical center in relation to the ground level (m);
- α_v - half of the vertical field of view (°);
- α_u - half of the horizontal field of view (°);
- θ_0 - the pitch angle of the camera (°).

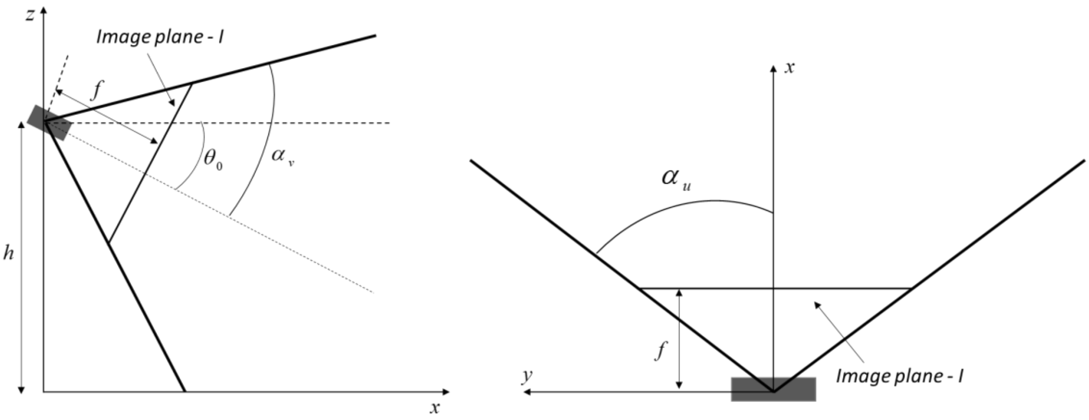

(a) **(b)**

Figure 3. (a) Lateral view and (b) top view of Figure 1.a

Considering a flat highway, the $f : I \to W$ is given by:

$$x(r) = h\left(\frac{1+\left[1-2\left(\frac{r-1}{M-1}\right)\right]\tan\alpha_v \tan\theta_0}{\tan\theta_0 - \left[1-2\left(\frac{r-1}{M-1}\right)\right]\tan\alpha_v}\right)$$

$$y(r,c) = h\left(\frac{1+\left[1-2\left(\frac{c-1}{N-1}\right)\right]\tan\alpha_u}{\sin\theta_0 - \left[1-2\left(\frac{r-1}{M-1}\right)\right]\tan\alpha_v \cos\theta_0}\right) \qquad (1)$$

$$z(r,c) = 0$$

Where:

$M \times N$ - Image resolution in pixels;

(r,c) - Image coordinates in pixels.

The inverse transform $g : W \longrightarrow I$, which generate an image without the perspective effect, is given by:

$$r(x) = \frac{M-1}{2}\left(1+\frac{h - x\tan\theta_0}{h\tan\theta_0 + x}\cot\alpha_v\right)+1$$

$$(2)$$

$$c(x,y) = \frac{N-1}{2}\left(1-\frac{y}{h\sin\theta_0 + x\cos\theta_0}\cot\alpha_u\right)+1$$

2.1 Camera parameters determination

The technical specifications of the cameras usually provide the values of the diagonal field of view ($2\alpha_d$) and the resolution ($M \times N$). However, as previously shown to compute IPM, it is necessary to know the values of α_v and α_u. From Figure 4 is possible to determine the relationship between the halve-angles of the fields of view and the resolution, which is shown in Eq. (3).

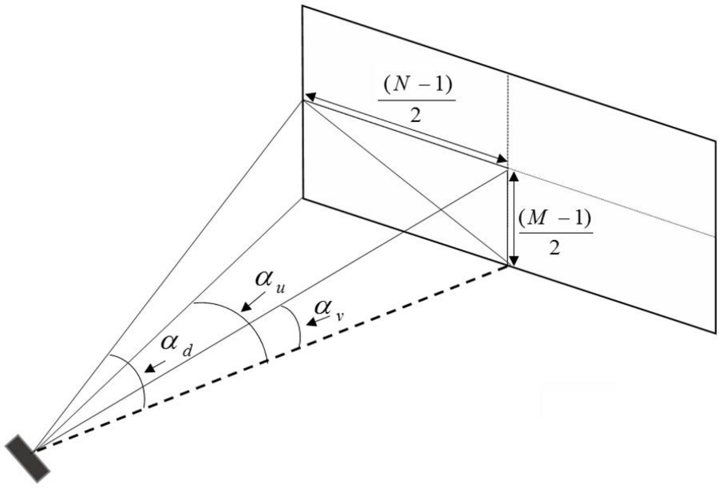

Figure 4. Relationship between halve-angles of fields of view and resolutions

$$\alpha_u = \tan^{-1}\left(\frac{N-1}{\sqrt{(M-1)^2+(N-1)^2}}\tan\alpha_d\right)$$

$$\alpha_v = \tan^{-1}\left(\frac{M-1}{\sqrt{(M-1)^2+(N-1)^2}}\tan\alpha_d\right) \tag{3}$$

2.2 IPM calibration

The slope of the highway ahead of the car and the camera position with respect to the W coordinates affect the IPM computation (Zhang et al, 2014). To correct the distortion produced by these conditions, the computation of the IPM is making using the pitch angle determined by:

$$\theta_0 = \tan^{-1}\left(\left(1-2\frac{r_h-1}{M-1}\right)\tan\alpha_v\right) \tag{4}$$

where (r_h, c_h) is, respectively, the row and column coordinates of the perspective image where parallel lane marks of the highway meet in the horizon (Fig. 5). This point, called vanishing point (VP), was located using the Hough Transform (Nieto et al., 2007).

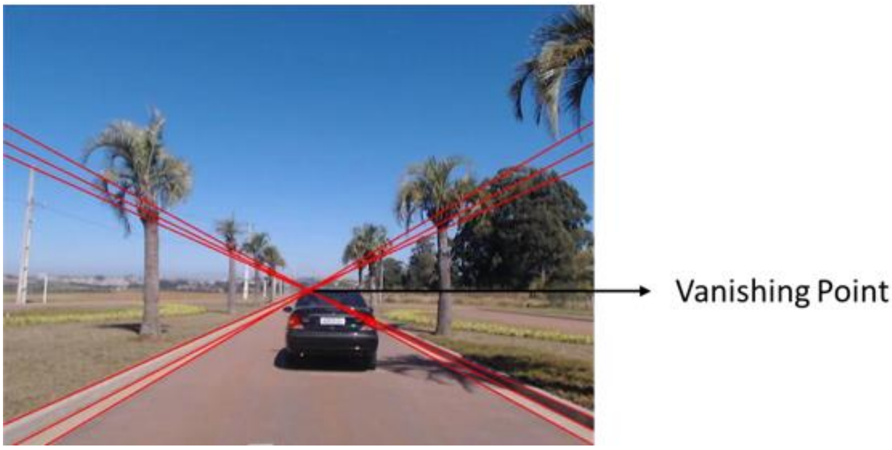

Figure 5. The vanishing point

The IPM calibration is done by fine-tuning of the camera height value (h) until the distance between two marks made on the highway (Fig. 6), obtained using Eq. (1), coincides with the known length D.

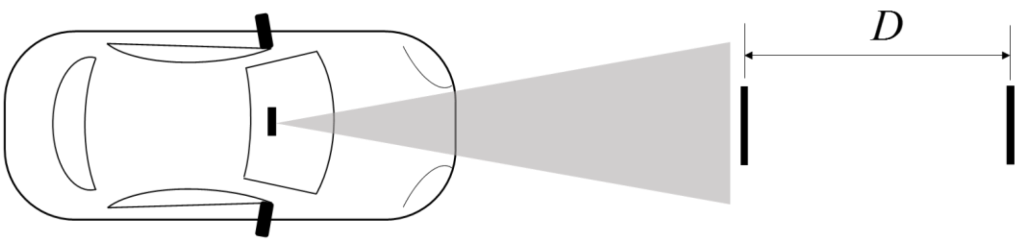

Figure 6. Marks made on the highway for IPM calibration

3 THE DISTANCE MEASUREMENT STRATEGY

The strategy proposed for measure an ahead vehicle distance based on a monocular camera is presented in Fig. 7. This strategy developed in MATLAB® (Mathworks®) consists of five stages: image acquisition and camera parameter definition, preprocessing, vanishing point and object detection and distance estimation.

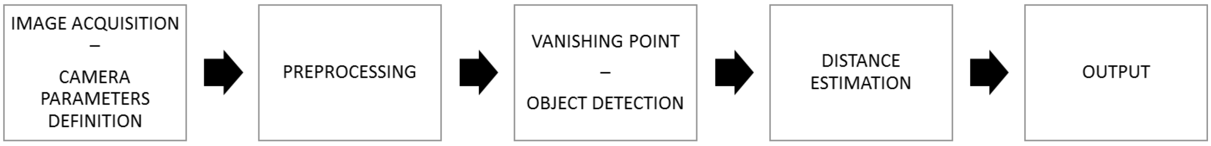

Figure 7. Strategy for measure an ahead vehicle distance based on a monocular camera

3.1 Image Acquisition and Camera Parameter Definition

The Logitech C920 camera installed in a vehicle windshield captured the images with the resolution of 1920x1080 pixels and 30 frames per second (fps). The CANape (Vector Informatik GmbH) with its optional Driver Assistance read these data from vehicle ECU and re-dimension the images to 640x480 pixels. This change in image format produces a new diagonal field of view ($2\alpha_d$) that was obtained by CANape. In general, the calculation of the halves angles of vertical and horizontal fields of view is done only once and were determined as shown in section 2.1.

3.2 Preprocessing

In this stage, the first step is the conversion of the acquired RGB image in grayscale (Fig. 8). This maps a three-layer input matrix in a single-layer matrix and therefore reduces the information amount to be manipulated. The grayscale image yet maintains important information necessary to the next step; the edge highlighted detection (Solomon & Breckon, 2011).

The Figure 8.c shows the binary image resulting from edge detection using the canny filter. This is the algorithm employed for edge detection because it satisfies three basics criteria (Canny, 1986; Andrade et al., 2017):

- Good detection. There are low rates of false positives and false negatives in edge detection.
- Good localization. The points detected as edges should be as close as possible to the true edge.
- A single response to each edge.

(a) **(b)** **(c)**

Figure 8. (a) An acquired RGB image is converted to (b) grayscale image and (c) the edges are detected using canny filter.

3.3 Vanishing Point and Object Detection

In this stage, the Hough transform (Fig. 9.a) makes the line fitting to the edges of the highway highlighted by the canny filter. In the sequence is found the vanishing point and the pitch angle of the camera installation, as seen in section 3.2 about IPM Calibration. Also using the vanishing point coordinate, the gray image (Fig. 9.b) is cropped slightly above the VP to allow the correct detection of vehicles near it. The grayscale image is used for detecting the vehicle which the active contour is applied.

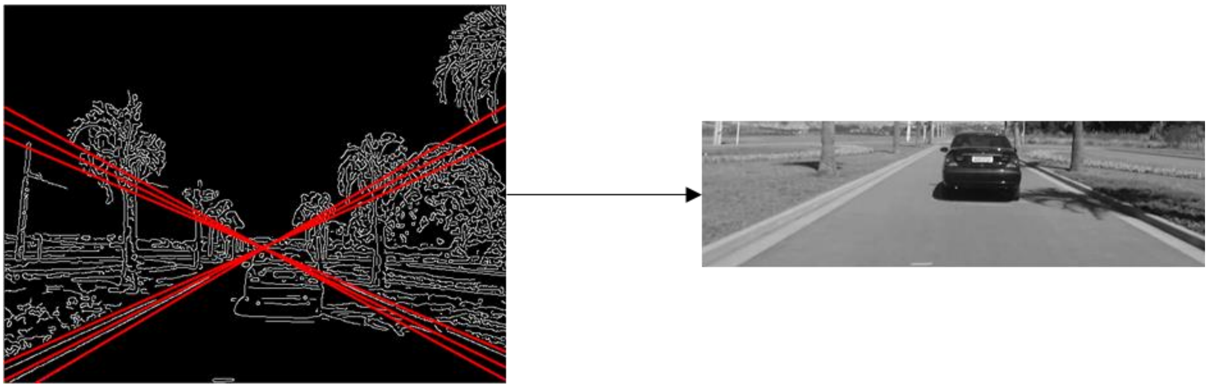

(a) **(b)**

Figure 9. (a) Vanishing point detected by Hough transform and (b) the result from cropping the image slightly above the VP to allow the correct detection of vehicle

Active contour model (ACM) or Snakes (Kass et al., 1987) is the method employed to detect the vehicle. The ACM minimizes the spline energy in order to extract important characteristics of the image, such as the object edges. An initial curve (Fig. 10.a), in blue) is manually drawing outside a target object. Then, the ACM deforms the curve toward the edge of the vehicle (Fig. 10.a, in red). The deformation of the curve is influenced by internal forces of the curve and by external forces that depart from the image (Rebouças et al., 2013). Identifying the vehicle region the ACM segments the image showing the area corresponding to the vehicle (Fig. 10.b).

(a) **(b)**

Figure 10. Active contour model applied to detect a vehicle: (a) in blue initialization curve and in red the detected vehicle edge and (b) the area corresponding to the vehicle.

3.4 Distance estimation

After the vehicle detection, the region of interest (ROI) to distance measurement is determined as shown in Fig. 11. Then the distance of the ahead vehicle is determined remapping the pixels by computing the x value by the Eq. 1.

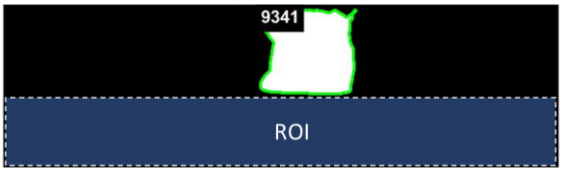

Figure 11. Region of interest (ROI) to distance measurement

Whenever necessary or if it is the first measurement, the calibration of the IPM through fine-tuning of his performed as shown in section 3.2. Figure 12 shows the aerial view resulting from IPM calibration process. Two distant D = 5m marks were made on the highway, one at 10m and the other at 15m. The distance measured in the IPM calibration process was 5,03m.

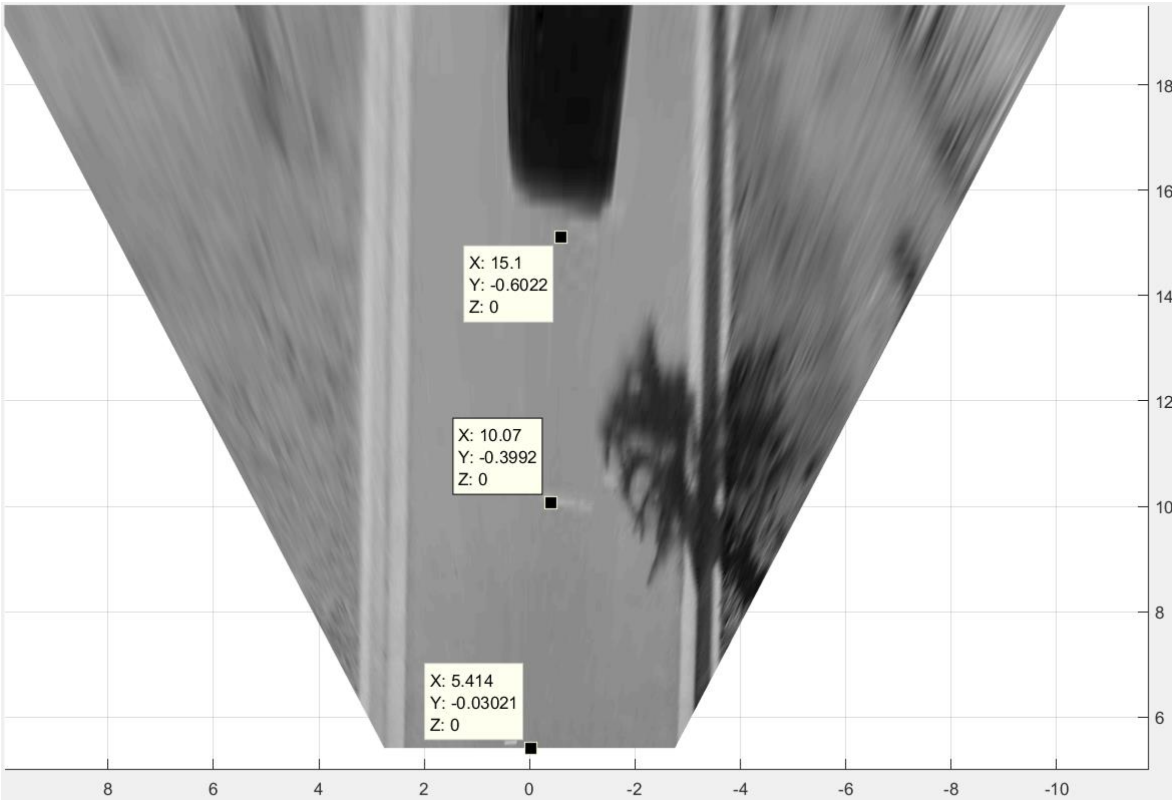

Figure 12. Aerial view resulting from IPM calibration process

4 RESULTS AND DISCUSSION

The distance measurement system using IPM was evaluated for a flat highway, with a vehicle positioned at distances between 10 and 50 meters from the camera, the measurements were taken every 5 m. For the correct positioning of the vehicle ahead, markings were made on the highway as shown in Fig. 13. A plumb level was used to ensure that the end of the vehicle's rear bumper matches the marking.

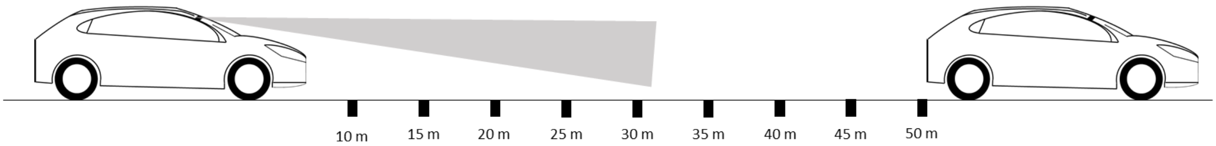

Figure 13. Markings made in the highway for distance measurement system evaluation.

The images have been acquired in August, at three periods of the day (Fig.14), in the mid-day (12 p.m.), in the mid-afternoon (4 p.m.) and the evening (7 p.m.). For each vehicle positioning, 200 measurements were taken.

(a) **(b)** **(c)**

Figure 14. Example of acquired images (a) in the mid-day, (b) in the mid-afternoon and (c) in the evening.

The mean errors of the measured distances ranged from 2.87% (at 12 p.m. and for 40m) to 18.43% (at 16 p.m. and for 50m) relative to the values accepted as true (Table 1). The mean errors in mid-afternoon and the evening were greater than that in the mid-day. By the analysis of variance method (ANOVA) with $F_{critical} = 3.01$, it was verified that, except for the distance of 10m, the average of the distances calculated in the 3 periods of the day are significantly different $(F_{calculated} > F_{critical})$. However, for a more adequate statistical analysis, it is necessary to take further distance measurements in other months of the year and at others periods of the day, including in the morning and at the night with artificial lighting.

Table 1. Coefficients in constitutive relations

	Mid-day 12 p.m.		Mid-afternoon 4 p.m.		Evening 7 p.m.		ANOVA ($F_{critical} = 3.01$)
	Distance (m)	Error %	Distance (m)	Error %	Distance (m)	Error %	$F_{calculated}$
10m	10.60±0.11	6.02	10.61±0.38	6.05	10.61±0.10	6.09	0.04
15m	15.65±0.09	4.32	16.48±0.00	9.89	16.31±0.15	8.71	3699.15
20m	20.71±0.20	3.56	21.14±0.00	5.72	21.42±0.27	7.12	701.67
25m	26.84±0.14	7.35	27.63±0.25	10,52	27.78±0.28	11.1	958.31
30m	31.62±0.16	5.41	33.57±0.63	11,9	32.98±0.44	9.93	960.45
35m	36.66±0.55	4.73	38.40±0.33	9,71	38.38±0.40	9.67	1055.09
40m	41.15±0.95	2.87	44.25±0.28	10,63	44.21±0.41	10.,52	1636.44
45m	47.22±1.19	4.93	50.85±1.41	13,01	51.79±0.73	15.08	844.74
50m	53.29±1.59	6.57	59.21±1.10	18,43	56.50±1.78	12.99	762.31

Figure 15.a shows the result of the edge detection using the canny filter on the image acquired near the mid-day (Fig. 14.a). Note that the vehicle's shadow is slightly ahead of the

marking made on the highway, probably because that the Sun is not exactly above the vehicle. Figure 15.b shows that the ACM in the grayscale image includes the shadow as part of the vehicle. The Fig. 15.c shows the aerial view obtained by IPM with the results of the distance measured; note the shadow in front of the mark made on the highway.

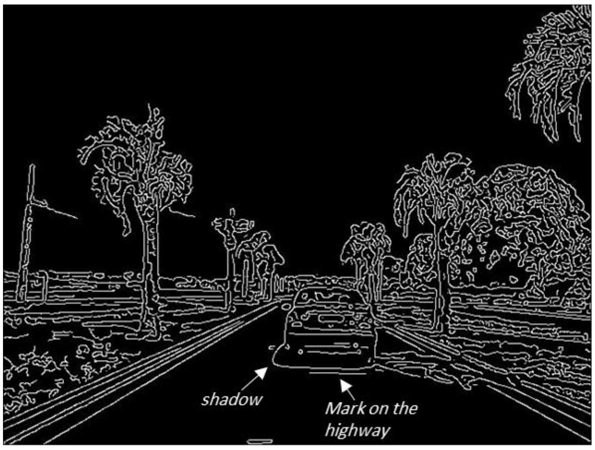

(a) **(b)**

(c)

Figure 15. The influence of shadow in the distance measurement realized in August and near the mid-day (a) the edge detection using the canny filter in the image of Fig. 14.a, (b) the vehicle detection using active contour method and (c) aerial view obtained by IPM with the results of the distance measured by the system.

Figure 16.a shows the result of the edge detection using the canny filter in the image acquired at 4 pm (Fig. 14.b). In this time the vehicle’s shadow is lateral and with a small slope due the Sun’s position. Note also that the right side of the shadow is due to the right rear wheel. The Fig. 16.c shows the aerial view obtained by IPM with the results of the distance measured, note the shadow is more distant than the mark makes on the highway.

The analysis of the Figures 15 and 16 results that the active contour method can only obtain a correct distance measure if the projection of the vehicle’s shadow on the highway coincides exactly with the beginning of rear bumper.

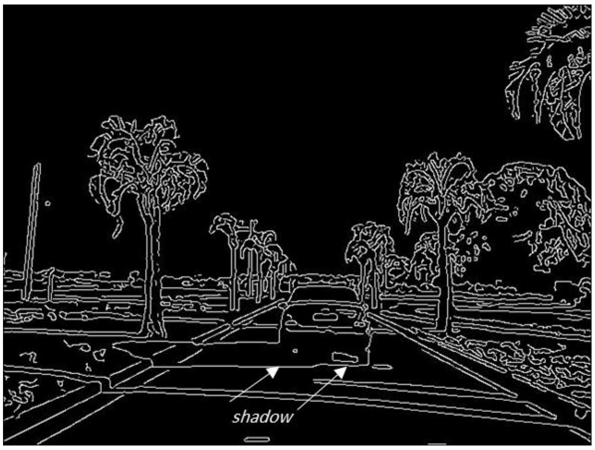

(a) **(b)**

(c)

Figure 16. The influence of shadow in the distance measurement realized in August and at 4 pm (a) the edge detection using the canny filter in the image of Fig. 14.b, (b) the vehicle detection using active contour method and (c) aerial view obtained by IPM with the results of the distance measured by the system.

5 CONCLUSION

The purpose distance measurement strategy presented satisfactory results. Through the results presented in Table 1 and the analysis of the images acquired and processed, we conclude that the measurement errors were caused by the environmental lighting conditions, the positioning of the vehicle relative to the light source, which produced different types and sizes of shadows that interfere with vehicle detection system. A limiting factor of the proposed strategy is the manual initialization of the active contour method. In the next step, we will evaluate methods such as that proposed by Lai and Chin (1993) which initializes the ACM efficiently and reliably using the Hough transform. Therefore, it is necessary the use or development of more robust and automated methods for vehicle detection to remove the influence of environmental conditions.

ACKNOWLEDGEMENTS

The authors are grateful for the support provided by the Graduation Program in Electrical Engineering of Federal University of Technology – Paraná – Ponta Grossa (UTFPR-PG) and by Fiat Chrysler Automobiles (FCA).

For their contributions, our special thanks to:

- João Henrique Zander Neme, Erick Margraf, William Takeshi Omoto and Ângelo Marcelo Tusset, members of the Laboratory of Automotive Systems (LSA, Laboratório de Sistemas Automotivos); and
- Rodrigo Amaral, Arthur Costa Ventura and Saulo Saulo Carvalho, collaborators of Fiat Chrysler Automobiles.

REFERENCES

Adamshuk, R., Carvalho, D., Neme, J. H., Margraf, E., Okida, S., Tusset, A., Santos, M. M., Amaral, R., Ventura, A. & Carvalho, S., 2017. On the applicability of inverse perspective mapping for the forward distance estimation based on the HSV colormap. *In Industrial Technology (ICIT), 2017 IEEE International Conference on*, pp. 1036-1041. IEEE.

Andrade, D., Adamshuk, R., Omoto, W., Franco, F., Neme, J. H., Okida, S., Tusset, A., Amaral, R., Ventura, A. & Santos, M. M. D., 2017. Lane Detection Using Orientation of Gradient and Vehicle Network Signals. *SAE Technical Paper*.

Bosch, 2012. Bosch stereo video camera enhances comfort and safety. Drive assistance systems make driving easier. [Online] Available: <http://www.bosch-presse.de/pressportal/de/en/bosch-stereo-video-camera-enhances-comfort-and-safety-41988.html> Accessed in: August 2017.

Broggi, A., 1995. A massively parallel approach to real-time vision-based road markings detection. In *Proceedings of the Intelligent Vehicles' 95 Symposium*, pp. 84-89. IEEE.

Canny, J., 1986. A computational approach to edge detection. IEEE Transactions on pattern analysis and machine intelligence, v.6, pp. 679-698.

Cario, G., Casavola, A., Franze, G., Lupia, M., Brasili, G., & it SpA, I., 2009. Predictive time-to-lane-crossing estimation for lane departure warning systems. In *Proceedings of the 21st International Technical Conference on the Enhanced Safety of Vehicles (ESV*).

IPEA, 2015. Acidentes de trânsito nas rodovias federais brasileiras: caracterização, tendências e custos para a sociedade. Instituto de Pesquisa Econômica Aplicada – IPEA.

Johnson, E.; Hamburger, R., 2007. CS5320/6320 Computer Vision Class Project. [Online] Available: < http://www.eng.utah.edu/~hamburge/>. Accessed in: October. 2016

Kass, M., Witkin, A., & Terzopoulos, D., 1988. Snakes: Active contour models. *International journal of computer vision*, vol. 1, n 4, pp. 321-331.

Lai, K. F., & Chin, R. T., 1993. On regularization, formulation and initialization of the active contour models (snakes). In *Asian Conference on Computer Vision*, pp. 542-545.

Nedevschi, S., Danescu, R., Frentiu, D., Marita, T., Oniga, F., Pocol, C., Schmidt, R & Graf, T., 2004. High accuracy stereo vision system for far distance obstacle detection. In *Intelligent Vehicles Symposium, 2004* IEEE, pp. 292-297.

Nieto, M., Salgado, L., Jaureguizar, F., & Cabrera, J., 2007. Stabilization of inverse perspective mapping images based on robust vanishing point estimation. *In Intelligent Vehicles Symposium, 2007 IEEE*, pp. 315-320. IEEE.

Rebouças Filho, P. P., Cortez, P. C., da Silva Félix, J. H., da Silveira, T., & Cavalcante, M. A. H. , 2013. Modelo de Contorno Ativo Crisp Adaptativo 2D aplicado na segmentação dos pulmões em imagens de TC do tórax de voluntários sadios e pacientes com enfisema pulmonar. *Rev. bras. eng. biomed*, vol. 29, n. 4, pp. 363-376.

Solomon, C., & Breckon, T., 2011. Fundamentals of Digital Image Processing: A practical approach with examples in Matlab. John Wiley & Sons.

Tuohy, S., O'Cualain, D., Jones, E., & Glavin, M., 2010. Distance determination for an automobile environment using inverse perspective mapping in OpenCV. *IET Irish Signals and Systems Conference (ISSC 2010)*, pp. 100–105.

World Health Organization, 2015. Global status report on road safety 2015. World Health Organization. [Online] Available: <http://www.who.int/violence_injury_prevention/road_safety_status/2015/en/>. Accessed in: October. 2016.

Zhang, D., Fang, B., Yang, W., Luo, X., & Tang, Y., 2014. Robust inverse perspective mapping based on vanishing point. In *Security, Pattern Analysis, and Cybernetics (SPAC), 2014 International Conference on*, pp. 458-463. IEEE.

Zhao, M., Mammeri, A., & Boukerche, A., 2015. Distance measurement system for smart vehicles. *New Technologies, Mobility and Security (NTMS), 2015 7th International Conference on*. IEEE.